Hindawi
Advances in Materials Science and Engineering
Volume 2020, Article ID 4198010, 15 pages
https://doi.org/10.1155/2020/4198010

Research Article

Research on Cutting Characteristics of Rock Plate with Two Sides Fixed and Two Sides Free

Zhenguo Lu,[1] **Qingliang Zeng**,[2,3] **Zhihai Liu**,[1] **Guanshun Gao**,[2] **and Peisi Zhong**[2,4]

[1]*College of Transportation, Shandong University of Science and Technology, Qingdao 266590, China*
[2]*College of Mechanical and Electronic Engineering, Shandong University of Science and Technology, Qingdao 266590, China*
[3]*College of Information Science and Engineering, Shandong Normal University, Jinan 250358, China*
[4]*Advanced Manufacturing Technology Center, Shandong University of Science and Technology, Qingdao 266590, China*

Correspondence should be addressed to Zhihai Liu; zhihliu@sdust.edu.cn

Received 19 August 2020; Revised 6 October 2020; Accepted 14 October 2020; Published 24 October 2020

Academic Editor: Baozhong Sun

Conical pick wear is an urgent problem in the roadway excavation caused by hard rock difficult to break. The traditional method of increasing cutting power to improve cutting performance of conical pick significantly increases pick wear. In the paper, a saw blade and conical pick combined cutting method is proposed based on increased free surface. To research the fracture morphology and cutting force of rock plate, theoretical, numerical, and experimental methods are used. By theoretical research, the bending mechanical model of rock plate bending is established. The cutting position and the junction between the free sides and fixed sides are preferentially broken. A numerical model combining the erosion and damage constitutive model is built, and the cutting process of rock plate was presented. According to rock plate experiment, the peak cutting force increases with the increasing uniaxial compressive strength, thickness of rock plate, and cutting depth of conical pick and decreases with the increasing width and height of rock plate. Exponential relationships exist between peak cutting force and thickness, width and height of rock plate, and cutting depth of conical pick. Linear relationship exists between peak cutting force and uniaxial compressive strength. The size of rock fragments increases with uniaxial compressive strength, width, and height of rock plate.

1. Introduction

Roadheader is the main engineering machinery for roadway excavation. As the main cutting tool, conical pick wear frequently occurs in the driving process of rock roadway, especially when encountering hard rock. The increase of pick wear leads to the increased cost of roadway excavation. Besides, the rock cutting efficiency is markedly reduced. The research of rock cutting has great significance for guiding production.

Considerable researches have been carried out on the interaction between rock and cutters. The most classical theory is proposed by Evans [1], who proved that tensile and compressive strength of rock and cutting depth of cutter are the major factors influencing cutting performance. Evans also pointed out that when the cone angle of conical pick decreased to zero, the cutting force was not equal to zero. Therefore, his cutting theory had defects, and it is hoped that other scholars can solve the problem. Goktan [2] and Roxborough and Liu [3] optimized the theory of Evans [1], taking into account friction angle between cutter and rock. Results demonstrated that the new theory was closer to the experimental results. Goktan and Gunes [4] carried out the full-scale tests to establish the equations to predict the cutting force and the equations suitable to the uniaxial compressive strength of rock within 30~170 MPa. Bilgin et al. [5] researched the relationship between cutting force and cutting parameters with 22 different property rocks and demonstrated that friction angle included in the cutting theory was more reasonable. Wang et al. [6] found that cone angle of conical pick had a significant influence on cutting force and specific energy and proposed the empirical prediction model. Triaxial testing apparatus was applied to research confining

pressure influencing conical pick cutting performance, and it was found that the cuttability of rock decreased and then increased with the increasing confining pressure [7]. Huang et al. [8] carried out numerical method to research the unidirectional confining pressure influencing cutting force, which was verified by experimental method. The fracture mode of rock with different cutting depth was investigated at the lower cutting depth. Rock presented ductile failure in lower cutting depth and brittle failure in higher cutting depth [9]. Based on indentation tests and Evans' cutting theory, a specific energy model was proposed that the fracture toughness, elasticity modulus of rock, and cutting depth of conical pick had significant influence on specific energy [10]. Zhao et al. [11] employed ANSYS/LS-DYNA to establish the interaction between spiral drum and rock, giving the stress distribution of spiral drum, and demonstrated that the main reason for coal and rock collapse was the interface between the broken rock and coal. Rock fragments formation at different cutting speeds was investigated through LS-DYNA, with the results showing that the finite element method was an effective method to research fragments separation [12]. Zhou and Lin [13] demonstrated that, with the cutting depth increasing, the rock failure was a process from ductile to brittle. Park et al. [14] combined experimental and numerical simulation to research the cutting efficiency of conical pick, with the results showing that compressive strength, cutting depth, and cutting angle had a significant influence on cutting performance of conical pick. Wang et al. [15] established the constitutive model between rock and conical pick, giving the relationship between cutting depth and specific energy, and the feasibility was illustrated by comparison with experiment. About pick wear, Dewangan et al. [16] employed scanning electron microscopy to research the pick wear mechanisms and found that the plastic deformation was one of the main reasons causing pick wear. Liu et al. [17] pointed out that high impact and stress caused the pick wear and that higher cutting angle was an effective method to reduce the point attack pick wear. Yang et al. [18], by establishing rotary cutting model of point attack pick, demonstrated that lower rotary angle and higher cutting angle were beneficial for reducing pick wear. Lu et al. [19–21] proposed a multi-free-surface-rock-cutting method under different constraints and carried out a numerical simulation study on cutting force in crushing process. Jeong et al. [22] used the smooth particle hydrodynamics (SPH) technique to build the rock and conical pick interaction mode and the Drucker-Prager model to simulate the brittle fracture. Su and Akkaş [23] researched the wear mechanism of two different types of conical picks and pointed out that metallurgical composition, pick position, and other environmental conditions had influence on wear mechanism. Liu [24] and Geng researched the influence of self-rotation on rock wear. Zhou et al. [25] combined theory and experiment to study dust generation in the process of rock breaking by pick, showing that the tip angle and attack angle had important influence on the dust generation. Zou et al. [26] used the discrete element method to study the influence of pick cutting parameters on rock fracture, showing that cutting depth and attack angle had significant influence on cutting force.

For the traditional rock cutting method, considerable researches have been carried out for rock cutting performance and pick wear with experimental and numerical simulation and theoretical methods. However, the new rock cutting method has seldom been related in past researches. In the paper, the diamond saw blade and conical pick combined rock cutting method is proposed. The research is based on rock plate formation. To predict the bending and preferential fracture position of rock plate, the theoretical research is proposed. The cutting process is studied by numerical simulation method. The experimental approach is carried out to research the fracture morphology and cutting force of rock plate.

2. Theoretical, Experimental, and Numerical Methods

2.1. New Rock Cutting Method. The new cutting method is mainly used to cut hard rock and solve the problems of lower rock cutting performance and pick wear in the traditional rock cutting method. The main implementation processes of the rock cutting method are as follows: (a) diamond saw blade is employed to slice kerf on the rock; thus the rock plate is formed and the strength of rock decreases obviously; (b) conical pick is used to cut the rock plate, as is shown in Figure 1(a). After the saw blade slices the rock, the rock plate's formation is with three sides fixed and one side free. During the rock plate cutting process, it is likely to form the rock plate with two sides fixed and two sides free as is shown in Figure 1(b) [19]. The research content of the paper is mainly based on the rock plate with two sides fixed and two sides free. The rock plate is cut by single point attack pick, and the cutting performance and rock fracture morphology are researched.

2.2. Theoretical Model. According to the reciprocity theorem of works [27–29], within the elastic range of rock plate, the sum of the work done by the first group of force and moment on the displacement generated by the second group of force and moment is equal to the sum of the work done by the second group of force and moment on the displacement generated by the first group of force and moment. Two different force systems are involved: one is defined as basic force system and the other as actual force system. In the paper, the basic bending system is the rock plate bending with four sides simply supported under the concentrated cutting force 1, as is presented in Figure 2(a); thus the system has some particularities. The actual bending system is the rock plate bending with arbitrary boundary conditions under the concentrated cutting force P, as is presented in Figure 2(b); thus the system has universality. The solution of the actual system should be based on the basic system.

Based on the reciprocity theorem, the relationship between the basic force system and the actual force system is presented in the following equation:

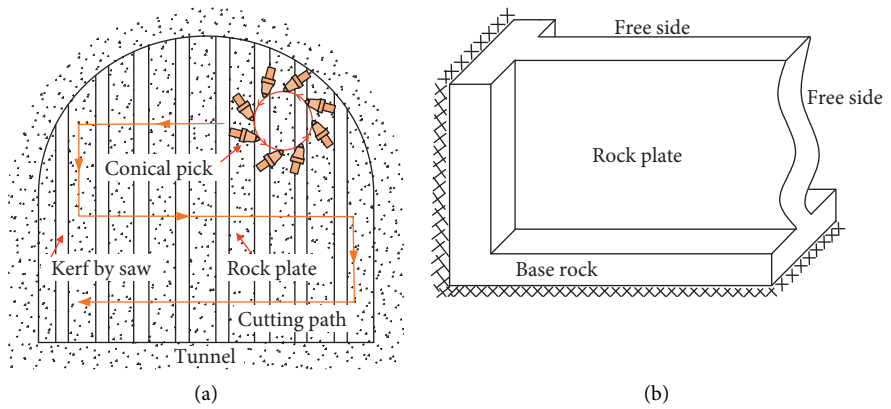

Figure 1: Rock cutting method based on multiple free surfaces formation. (a) Roadway tunneling sketch based on new cutting method. (b) Rock plate cutting with two sides fixed and two sides free.

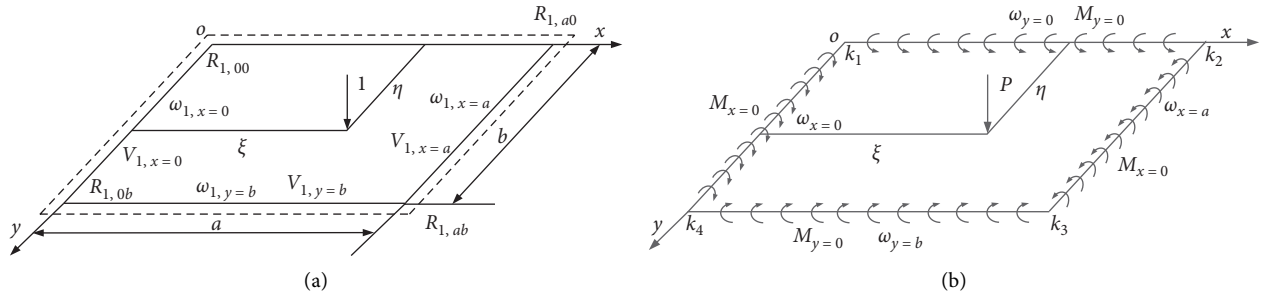

Figure 2: The force systems based on reciprocity theorem. (a) Basic system and (b) actual system.

$$\begin{aligned}\omega(\xi,\eta) &- \int_0^b V_{1,x=0}\omega_{x=0}\mathrm{d}y + \int_0^b V_{1,x=a}\omega_{x=a}\mathrm{d}y - \int_0^a V_{1,y=0}\omega_{y=0}\mathrm{d}x \\ &+ \int_0^a V_{1,y=b}\omega_{y=b}\mathrm{d}x - R_{1,00}k_1 + R_{1,a0}k_2 - R_{1,ab}k_3 + R_{1,0b}k_4 \\ &= P\omega_1(\xi,\eta) + \int_0^b M_{x=0}\omega_{1,x=0}\mathrm{d}y - \int_0^b M_{x=a}\omega_{1,x=a}\mathrm{d}y \\ &+ \int_0^a M_{y=0}\omega_{1,y=0}\mathrm{d}x - \int_0^a M_{y=b}\omega_{1,y=b}\mathrm{d}x,\end{aligned} \tag{1}$$

where a and b are the dimensions of rock plate, P is cutting force, $\omega(\xi, \eta)$ is the rock plate bending of actual force system, $\omega_1(\xi, \eta)$ is the rock plate bending of basic force system, (ξ, η) is cutting position of conical pick on the rock plate, M is the bending moment of each actual force system side, V is the shear force born by each side of basic force system, R is fulcrum resistance force of basic force system, and k is the fulcrum displacement of actual system.

The bending equation of rock plate is a function about cutting force, bending moment, and shear force. For the actual force system with specific boundary condition, the bending moment and the corresponding deflection can be assumed with trigonometric series to obtain the solution of $\omega(\xi, \eta)$. Through (1), it can be seen that the solution of $\omega(\xi, \eta)$ must be based on the solution of $\omega_1(\xi, \eta)$. The basic force system is a known system according to [27–29], and R, V, $\omega_1(\xi, \eta)$, and ω_1 in the basic force system are the known parameters.

The actual force system of the rock plate with two sides fixed and two sides free is presented in Figure 3(a). OA and OC are fixed sides, and AB and BC are free sides. The fixed boundary can be transformed to the combination of simple support and bending moment, as is presented in Figure 3(b).

According to (1), for the rock plate with two sides fixed and two sides free, the relationship between the basic force system shown in Figure 2(a) and the actual force system shown in Figure 3(b) is shown in the following equation:

$$\begin{aligned}\omega(\xi,\eta) = P\omega_1(\xi,\eta) &+ \int_0^b M_{x=0}\omega_{1,x=0}\mathrm{d}y + \int_0^a M_{y=0}\omega_{1,x=0}\mathrm{d}x \\ &- \int_0^b V_{1,}x = 0\omega_{x=a}\mathrm{d}y - \int_0^a V_{1,}y = b\omega_{y=b}\mathrm{d}x + R_B k_3.\end{aligned} \tag{2}$$

The boundary condition of rock plate with two sides fixed and two sides free is presented as follows:

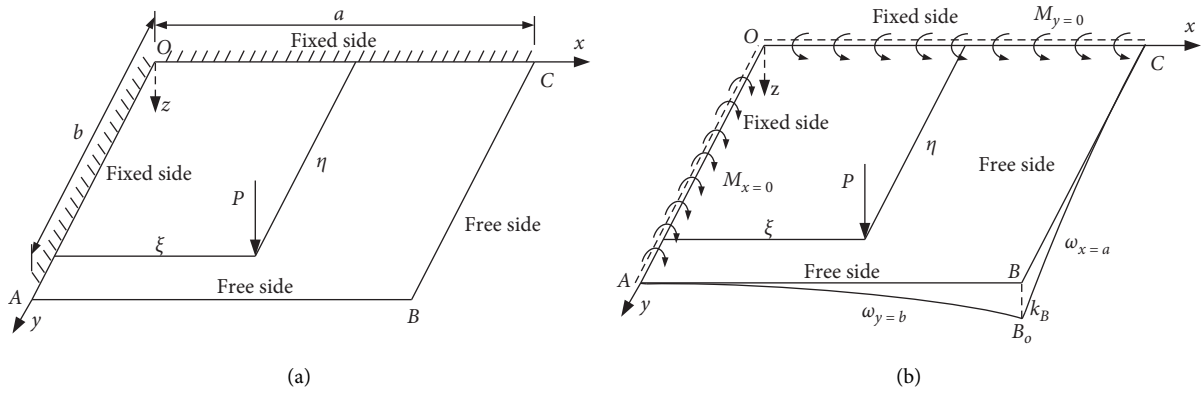

Figure 3: Mechanical models of rock plate with two adjacent sides clamped under concentrated load. (a) The actual force system and (b) equivalent system of actual system.

$$\left(\frac{\partial \omega}{\partial \xi}\right)_{\xi=0} = 0, \left(\frac{\partial \omega}{\partial \eta}\right)_{\eta=0} = 0, \left(V_{1,\eta}\right)_{\eta=b} = 0, \left(V_{1,\xi}\right)_{\xi=a} = 0, \left(\frac{\partial^2 \omega}{\partial \xi\, \partial \eta}\right)_{\substack{\xi=a \\ \eta=b}} = 0. \tag{3}$$

In order to solve the bending problem of rock plate, the following assumptions are made for bending moment and deflection of the actual force system:

$$\begin{cases} M_{x=0} = \sum_{n=1,2}^{\infty} A_n \sin \beta_n y, \\ M_{y=0} = \sum_{n=1,2}^{\infty} B_m \sin \alpha_m x, \\ \omega_{x=a} = \sum_{n=1,2}^{\infty} C_n \sin \beta_n y + k_B y, \\ \omega_{y=b} = \sum_{n=1,2}^{\infty} D_m \sin \alpha_m y + k_B x. \end{cases} \tag{4}$$

In (4), there are five unknowns of A_n, B_m, C_n, D_m, and K_B. By combining the five boundary conditions in (3), the unknowns can be solved.

According to actual working conditions, the conical pick generally acts on the free boundary of the rock plate. Taking $a = b$, $h/a = 0.1$, and $v = 0.3$, the cutting force P acting on midpoint of the free side with the coordinates is $(a, b/2)$. Due to one end fixed and one end free, the free side presents asymmetric bending. The deflection of the free side $x = a$ is shown in Figure 4(a), and the maximum reflection is $0.37\,(Pa^2/D)$ obtained at the cutting position, where D is the bending strength. The bending moment of fixed side $y = 0$ is presented in Figure 4(b), and the maximum bending moment is 1.08 $(-P)$, presented at the junction between free side and fixed side. Therefore, when cutting force P acts on the midpoint of the free side, the cutting position and the junction between free side and fixed side are preferential fracture.

2.3. Mechanical Properties Test and Rock Plate Cutting Test. Four different rock specimens are gathered to obtain the mechanical properties. To study rock property on rock cutting performance and to establish the numerical model, uniaxial compressive strength (UCS), elastic modulus (E), density (D), and tensile strength (T) are tested by electrohydraulic servo compression machine. The cylindrical specimens with dimensions of φ50 mm in diameter and 100 mm in height are used to conduct the compression test, and others with dimensions of φ50 mm in diameter and 50 mm in height are used to conduct the Brazilian splitting test. The compressive test is shown in Figure 5, and sample fracture result is shown in Figure 6. The strain-stress curve obtained from the compressive test is presented in Figure 7. UCS is the maximum stress of strain-stress curve, and E is obtained at the half of the maximum stress. The quality of the samples is measured; meanwhile, the volume of the sample can be calculated. Thus, D can be measured from quality divided by volume. In order to avoid the contingency of the results, tests are conducted three times for each mechanical property. The main properties of rock are shown in Table 1.

The rock plate cutting test bed consists of hydraulic system, rock cutting component, and signal acquisition system, as is shown in Figure 8. The working principles of rock plate cutting bed are the following: (a) The cylinder telescopes with control of hydraulic system control unit, with power provided by pumping station. (b) The rock plate is fixed on the rock plate fixture and moves on the sliding guide under the action of cylinder. (c) Thus, the moving rock plate is cut by the stationary conical pick. (d) The static torque sensor generates deformation under the action of rock cutting force and outputs the voltage signal in mV unit. (e) The voltage signal is amplified to V unit through transmitter. (f) The enlarged voltage signal is acquired by signal acquisition device and displayed on the computer. In the rock cutting process, the sampling frequency of signal acquisition device is 10 kHz. (g) The schematic diagram of signal acquisition system is shown in Figure 9.

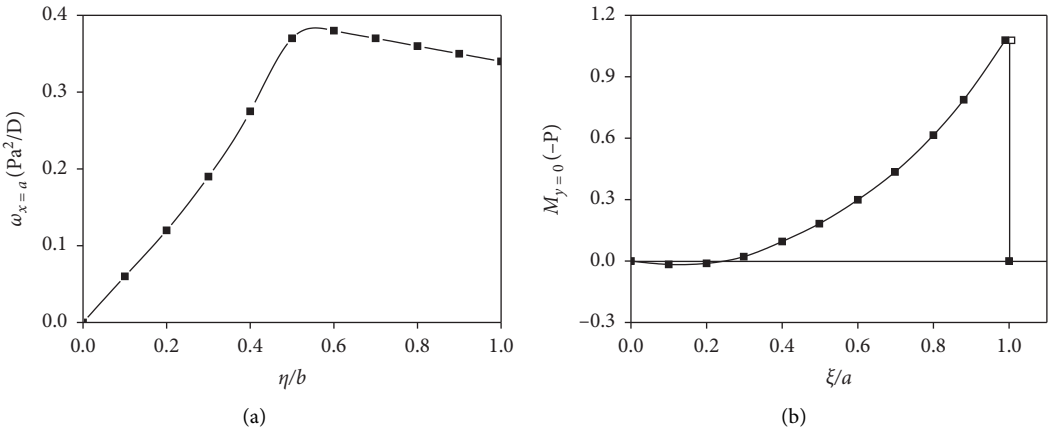

Figure 4: The deflection and bending moment with the concentrated cutting force (P) acting on (a, $b/2$): (a) the deflection on free side $x = a$ and (b) the bending moment on fixed side $y = 0$.

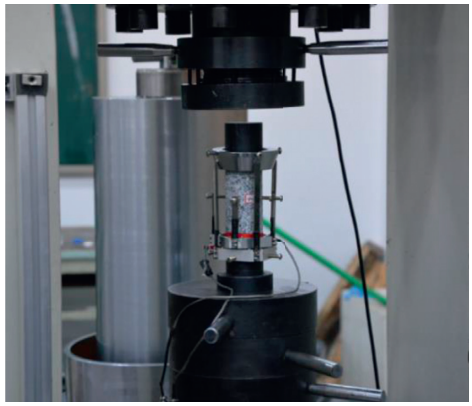

Figure 5: Compressive strength tested.

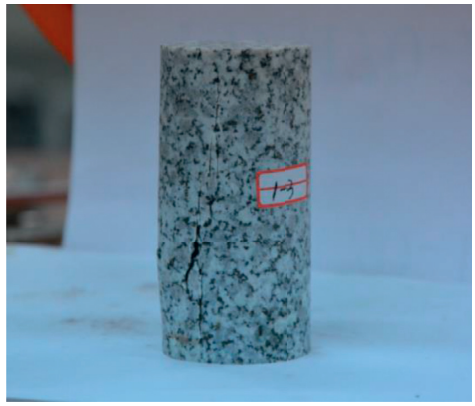

Figure 6: The compressed result.

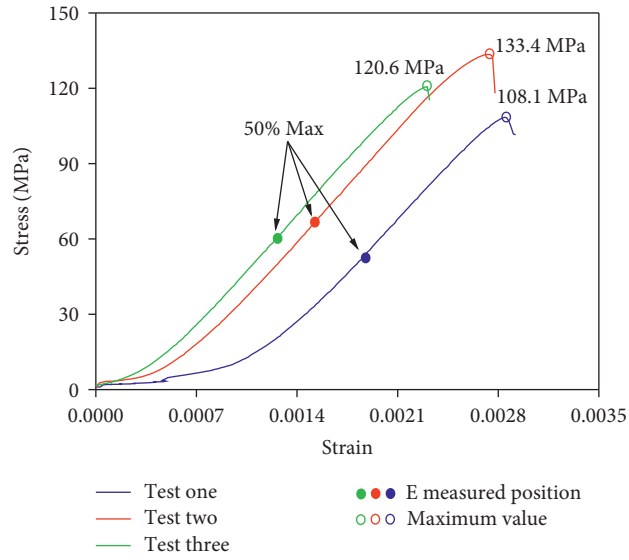

Figure 7: The stress-strain curve obtained from compression test.

Table 1: Mechanical properties of the rock.

Rock	UCS (MPa)	BTS (MPa)	E (GPa)	D (kg/m^3)
Granite	120.7	12.1	45.5	2732
Marble	43.8	5.3	52.9	2670
Sandstone-1	86.4	7.9	54.5	2683
Sandstone-2	139.1	10.6	58.3	2716

2.4. Numerical Model. Experiment is the most effective method to research rock cutting; it is difficult to present rock plate cutting process in the experiment detail. Consequently, numerical simulation is employed to study the rock cutting process. LS-DYNA is adopted to carry out numerical simulation. The model consists of rock and conical pick, and the rock consists of base rock and rock plate as is shown in Figure 10. The stationary rock is cut by the moved conical pick with the constant velocity. The bottom and left surfaces of the rock are fixed. *MAT_JOHNSON_HOLMQUIST_CONCRETE [30] is assigned to the rock plate. *MAT_ADD_EROSION and *CONTACT_ERODING_SURFACE_TO_SURFACE are defined to ensure crack generated and rock fracture. l_x, l_y, and l_z are the width, thickness, and height of rock plate, assigned by 500 mm, 20 mm, and 200 mm, respectively. θ is the cutting angle between conical pick velocity and y-axis, assigned as 0

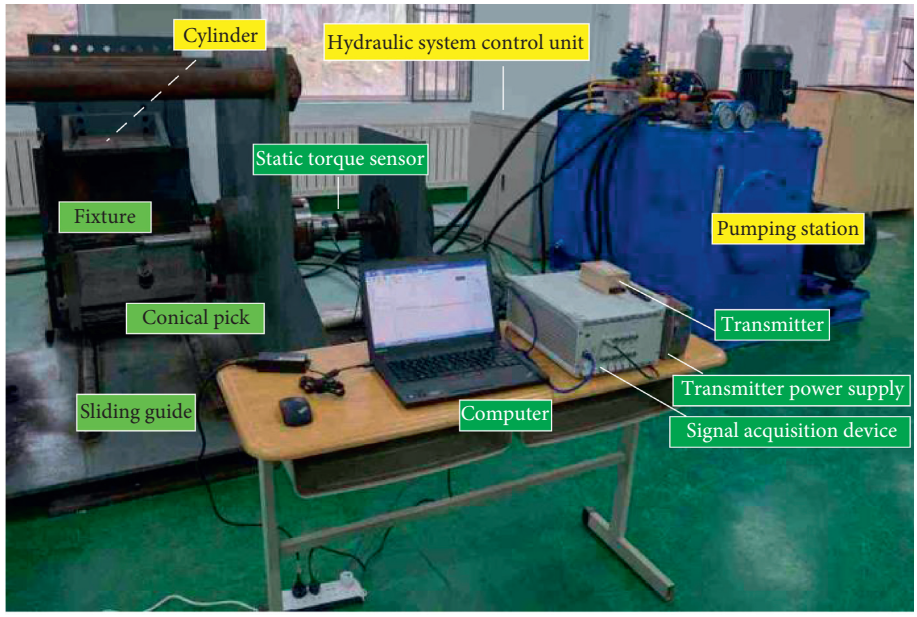

Figure 8: Rock plate cutting test bed.

degrees. In other words, the direction of pick velocity is the same as positive direction of y-axis. l_{xp}/l_x is defined as the cutting position, set as 0.5 in the paper. The hourglass energy and element penetration significantly affect the cutting force. In order to avoid the above phenomenon, the full integration algorithm is adopted in the numerical simulation. The impact angle and the tip angle of conical pick are 57° and 80°, respectively. Besides, the friction angle between the cutting pick and rock plate is assigned as 8.5° [5, 31]. The parameters of granite are shown in Table 2.

3. Results and Discussion

3.1. Rock Cutting Process. The cutting process of rock plate under the numerical simulation condition is shown in Figure 11. With the contact between conical pick and rock plate, rock elements failure around the cutting position under the pressure of conical pick is shown in Figure 11(a), with the main feature being initial crushing. This is mainly because the contact area between the cutting teeth and the rock is too small, and the rock can bear less force. As a result, the rock is compressed and destroyed at the contact position. With the increase of pressure between conical pick and rock plate, the rock plate breaks and generates crack along with the middle line of rock plate starting from the cutting position; meanwhile, crack also occurs at the junction of the left fixed side and free side, as is presented in Figure 11(b). The initial fracture position of rock plate is consistent with the theoretical result. After the initial crushing of the rock plate, the contact area between the pick and the rock plate increases, and the interaction force between the pick and the rock increases. The resulting cutting force makes the stress generated at the contact position greater, resulting in the rock plate cracking from the middle, and it also makes the bending moment at the junction of base rock and rock plate larger, resulting in tensile failure at this point. Afterwards, with the movement of the pick, the main crack is formed, dividing the rock plate into two pieces, and then the rock plate breaks at bottom and the junction between bottom fixed side and right free side is shown in Figure 11(c). This is mainly due to the deformation of the rock plate caused by the movement of the conical pick, and the tensile stress is formed in the middle of the rock plate, which makes the rock plate continue to fracture along the original crack. After the fracture reaches the bottom of the rock plate, a large bending moment is formed near the crack, and then cracks are generated along the boundary between the rock plate and the base rock. From now on, the rock plate breaks wholly. The existing cracks continue to expand under the action of pick until they are connected to each other inside and outside of rock plate, as is shown in Figure 11(d) and Figure 11(e). Subsequently, with rock plate separated from base rock, the cutting process of rock plate finishes.

3.2. UCS Influencing Cutting Performance. In the experiment, two sides of rock plate are fixed and two sides are free. The cutting results of rock plate with 200 mm height, 500 mm width, 20 mm thickness, and 20 mm cutting depth are shown in Figure 12. Cutting depth is defined as the distance from cutting position to the top side of rock plate. It can be seen that, with the difference of UCS, the fracture morphology of rock plate is significantly different. With the increasing UCS, the dimension of fragment obtained from rock plate cutting process increases, but the quantity of fragment decreases. All of the rock plate breaks at the bottom fixed side, and the fracture position extends to the right free side.

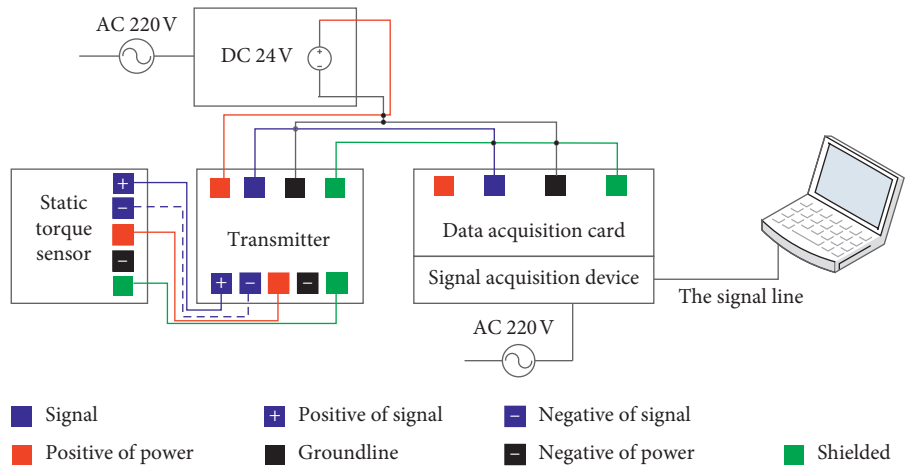

Figure 9: Schematic diagram of signal acquisition system.

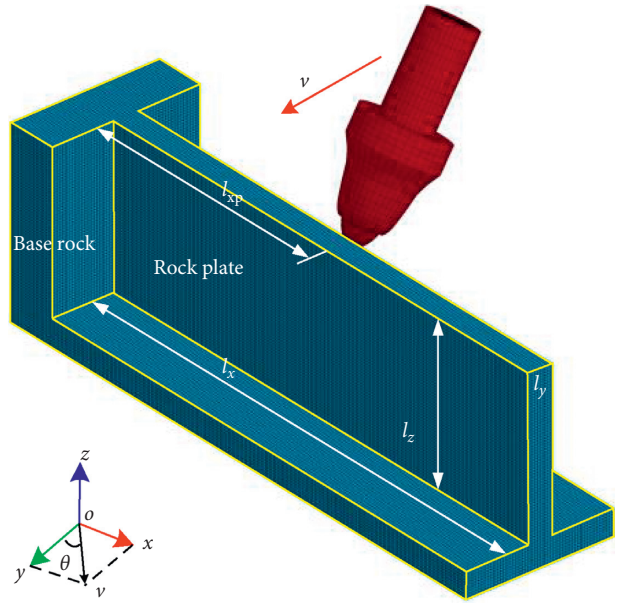

Figure 10: The numerical model between conical pick and rock plate.

Table 2: Parameters of JHC for granite.

R_o/kg·m^{-3}	G/Pa	A	B	C	N	F_c'/Pa	T/Pa	$\dot{\varepsilon}_0$	ε
2732	$20e^9$	0.79	1.6	0.007	0.61	$120.7e^6$	$12.1e^6$	$1e^{-6}$	0.01
$\sigma_{f,\ max}$	P_c/Pa	μ_c	P_{lock}/Pa	μ_{lock}	D_1	D_2	K_1	K_2	K_3
7	47.1	0.01	$8e^8$	0.1	0.04	1.0	$12e^9$	$25e^9$	$42e^9$

The cutting force for different rock properties with time is presented in Figure 13. It can be seen that the variation of cutting force is the same. However, for the rock with different properties, the peak cutting force (PCF) is obviously different. The PCF obtained in the experiment is illustrated in Table 3 and the variation in PCF with UCS is shown in Figure 14. The minimum PCF is 0.596 kN for marble with the least UCS, while the maximum PCF is 1.975 kN for sandstone-2 with the greatest UCS. PCF increases significantly with UCS. According to linear fitting, it can be seen that linear relationship exists between PCF and UCS. R^2 equal to 0.97356 indicates that the relevance is strong.

3.3. Thickness of Rock Plate Influencing Cutting Performance. The thickness of rock plate is an important factor that influences cutting force. The cutting force obtained at 500 mm width, 200 mm height, and thickness of 16 mm, 20 mm, 26 mm, and 30 mm is shown in Figure 15. With the different thickness of rock plate, the cutting force and PCF are

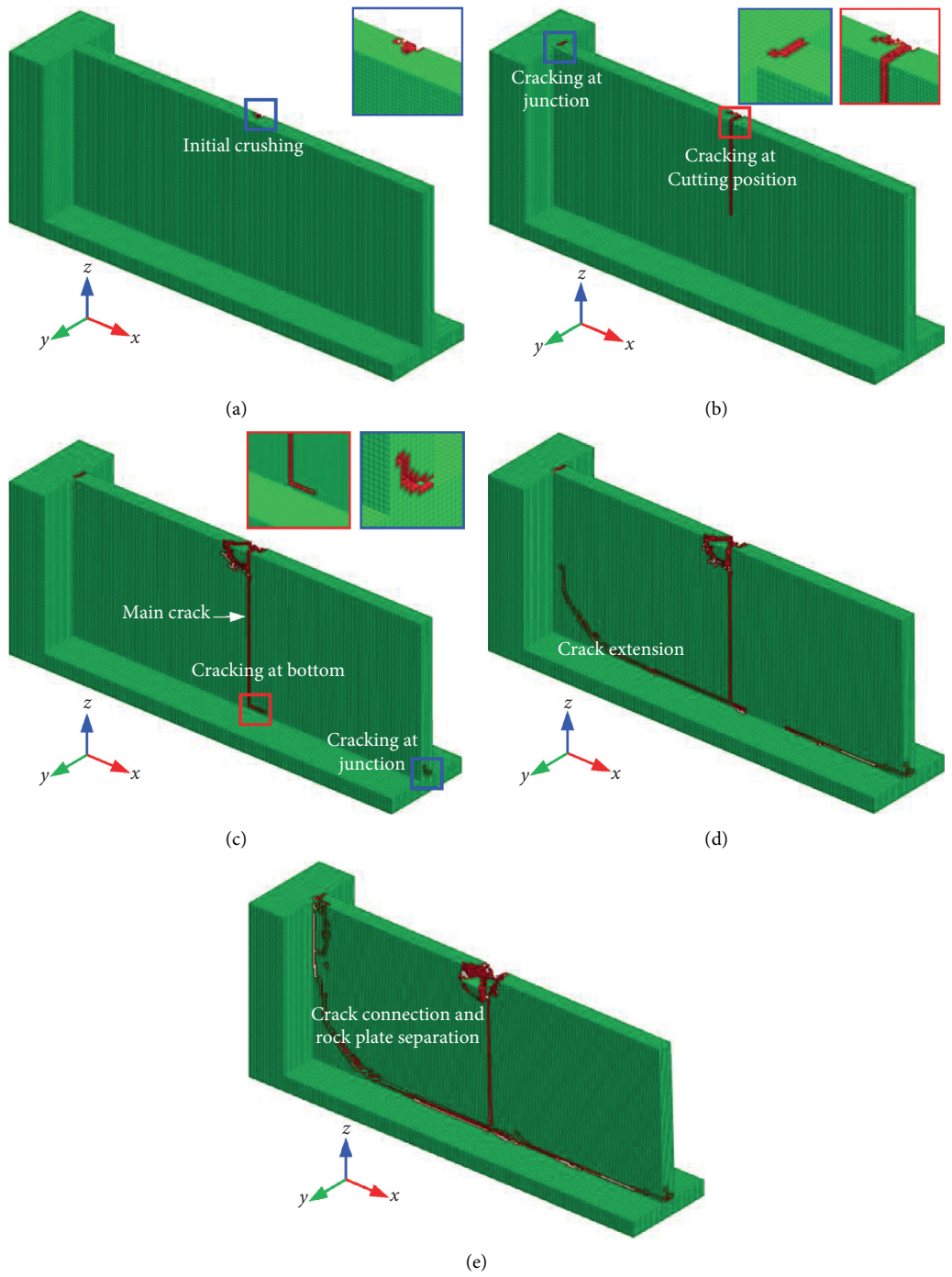

Figure 11: Rock plate cutting process. (a) Initial crushing. (b) Crack generation. (c, d) Crack extension. (e) Crack connection.

different. PCF with different rock plates is illustrated in Table 4. The PCF of 5.4664 kN is obtained at thickness of 30 mm, which is significantly greater than the 1.126 kN obtained at thickness of 16 mm. Although the difference of thickness is only 14 mm, the difference of PCF reaches 4.338 kN. It can be concluded that thickness of rock plate has a significant influence on cutting force, for the flexural strength of rock plate increases with the increasing thickness. In order to crush the rock plate with higher thickness, higher cutting force is required. The change tendency of PCF with thickness of rock plate is shown in Figure 16. PCF increases with the increasing thickness. The fitting results show that exponential relationship exists between peak cutting and thickness of rock plate. R^2 of 0.99158 shows that the exponential relationship is strong and credible.

3.4. Width of Rock Plate Influencing Cutting Performance. The cutting results of rock plates at thickness of 20 mm and width of 300 mm and 400 mm are shown in Figure 17. The

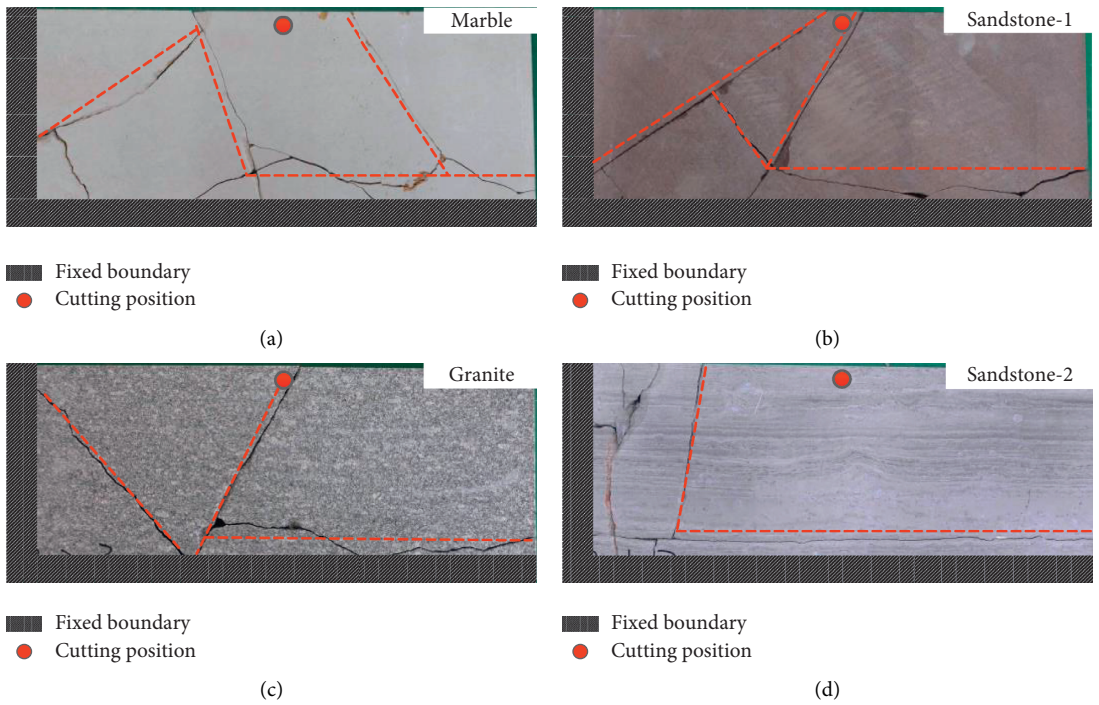

Figure 12: The cutting results of rock with different UCS. (a) Marble. (b) Sandstone-1. (c) Granite. (d) Sandstone-2.

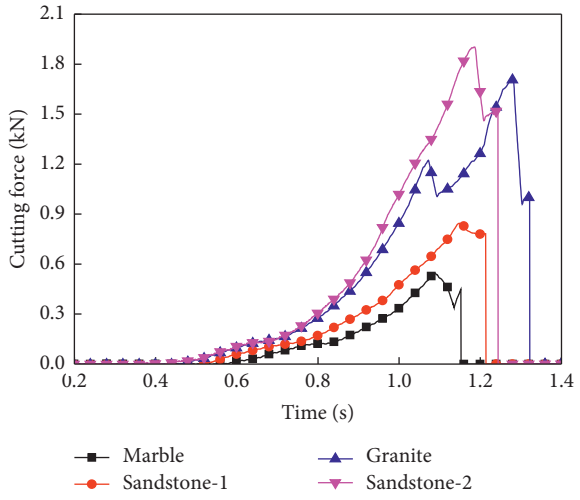

Figure 13: Variation in cutting force with time.

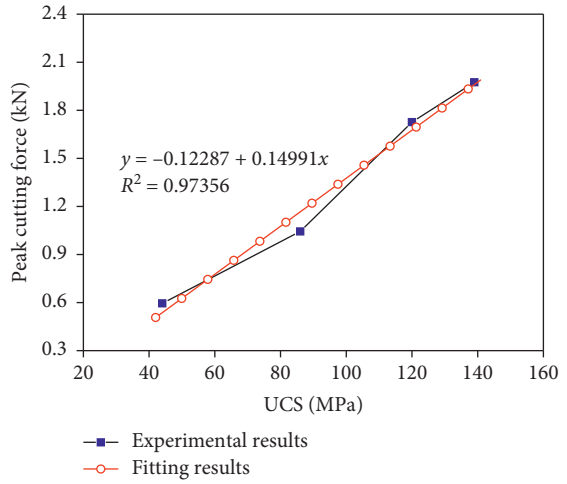

Figure 14: The relationship between PCF and UCS.

Table 3: The PCF with different UCS.

Rock	Marble	Sandstone-1	Granite	Sandstone-2
UCS (MPa)	43.8	86.4	120.7	139.1
PCF (kN)	0.596	1.004	1.726	1.975

rock plate fractures along the bottom side until the free side, and, on the left part of rock, two main random cracks are generated. The cutting result obtained at width of 300 mm is shown in Figure 17(a), and that of 400 mm is shown in Figure 17(b), basically with the same width of 500 mm shown in Figure 12(c). Especially for widths of 400 mm and 500 mm, the cutting results are the same. Therefore, the width of rock plate has little effect on rock plate fracture morphology on the condition of two sides fixed and two sides free.

The cutting force obtained at thickness of 20 mm, height of 200 mm, and width of 200 mm, 300 mm, 400 mm, and 500 mm is presented in Figure 18. The boundaries between each curve are confusing, significantly different from Figures 13 and 15. The reason is that the change regulation and PFC are similar in each cutting force. PCF with different width of rock plate and the relationship between PCF and width are shown in Table 5 and Figure 19. PCF decreases with the increasing width of rock plate, and when the width decreases to 300 mm, the peak cutting force becomes stable,

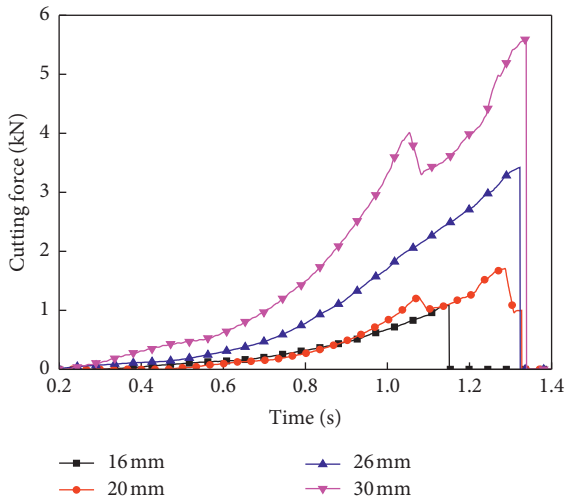

Figure 15: Variation in cutting force with time at different thickness.

Table 4: The PCF of granite with different thickness.

Thickness of rock plate (mm)	16	20	26	30
PCF (kN)	1.126	1.726	3.467	5.646

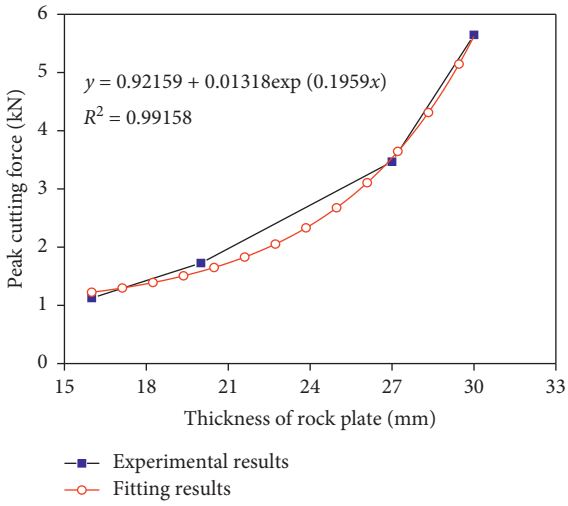

Figure 16: The relationship between PCF and thickness of rock plate.

no longer decreasing with the increasing width. At the widths of 200 mm and 500 mm, the peak cutting forces are 2.001 kN and 1.726 kN, respectively. When the width reduces by 300 mm, the corresponding cutting force decreases by 0.275 kN. It indicates that although the cutting force has a tendency of decrease, the amplitude is very small. Therefore, the width of rock plate has little influence on cutting force. From the fitting result in Figure 19, exponential relationship exists between width and PCF with R^2 of 0.98847.

3.5. Height of Rock Plate Influencing Cutting Performance. The cutting result of granite with width of 500 mm, thickness of 20 mm, and height of 80 mm and 120 mm is illustrated in Figure 20. At the height of 80 mm, the cutting result significantly differs from Figure 12(c) with 200 mm in height. The fracture area is mainly near the conical pick and relatively smaller when compared with Figure 12(c). Besides, the rock plates on the left and right sides are retained on the base rock. At height of 120 mm, the right part of rock plate breaks, with the decreased ratio between width and height and increased fracture area. Therefore, rock plate with higher ratio of width to height corresponds to smaller regional fracture.

The cutting force obtained at heights of 80 mm, 120 mm, 160 mm, and 200 mm is illustrated in Figure 21. At height of 80 mm, the value of cutting force is obviously bigger than that obtained at other heights. At heights of 120 mm, 160 mm, and 200 mm, little difference exists between the cutting forces. The statistics of PCF are given in Table 6 and the relationship between PCF and height of rock plate is shown in Figure 22.

The PCF of 2.559 kN obtained at height of 80 mm is still significantly greater than others. It is because lower height results in the lower distance between conical pick and bottom of rock plate. In order to obtain the same bending moment at bottom fixed side, lower distance corresponds to higher cutting force. At the height within 120 mm to 200 mm, although the cutting fore has the tendency to decrease, the value change is very small and basically stable. It is because when the height of rock plate increases, the cutting force depends on the distance between the cutting position and the left fixed boundary. Therefore, PCF decreases with the increasing height of rock plate and it remains stable until the height increases to a certain value. Exponential relationship exists between PCF and height of rock plate with R^2 of 0.9595 and P value of 0.02.

3.6. Cutting Depth Influencing Cutting Performance. The cutting results of rock plate with width of 500 mm, height of 200 mm, thickness of 20 mm, and cutting depth of 4 mm and 36 mm are shown in Figure 23. At the cutting depth of 4 mm, the rock plate fracture morphology is similar to cutting depth of 20 mm. At cutting depth of 36 mm, the cutting results have a significant difference with two others, with only half of rock plate breaking and the other half remaining on the base rock. The cutting force at different cutting depths is shown in Figure 24, with significant difference of cutting force for different cutting depths. At the higher cutting depth, the cutting force fluctuates during the rising process, for each part of rock plate does not break at the same time. PCF with different cutting depths is illustrated in Table 7. At cutting depth of 4 mm, the minimum PCF is obtained with the value of 1.853 kN. Relatively, at cutting depth of 45 mm, the maximum PCF is obtained with the value of 4.314 kN. The relationship between PCF and cutting depth for rock plate with two sides fixed and two sides free is shown in Figure 25. It is obvious that PCF increases significantly with the increasing cutting depth. From variation of numerical

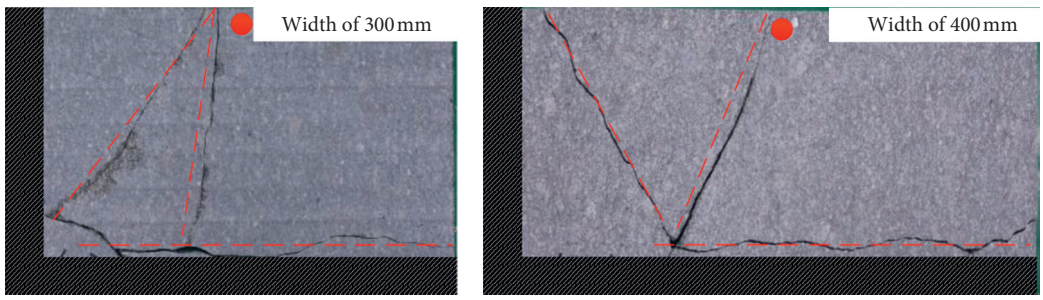

Figure 17: The cutting force at different thickness of rock plate. (a) 300 mm and (b) 400 mm.

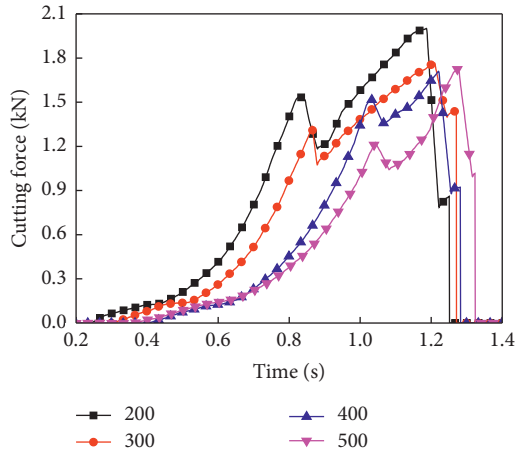

Figure 18: Variation in cutting force with time at different width.

Table 5: The PFC with different width of rock plate.

Width of rock plate (mm)	200	300	400	500
PFC (kN)	2.001	1.764	1.712	1.726

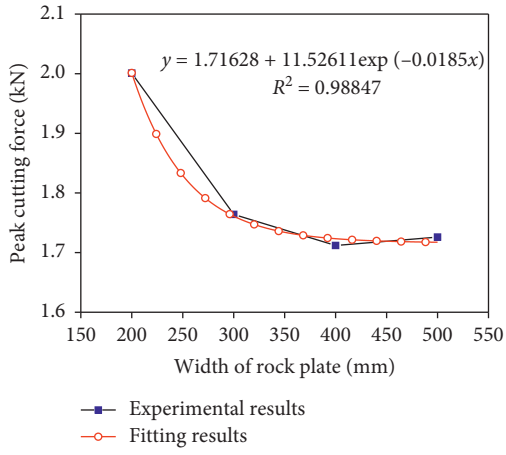

Figure 19: The relationship between PCF and width of rock plate.

value, cutting depth influences PCF greater than width and height of rock plate. The fitting results show that positive exponential relationship exists between PCF and cutting depth with R^2 of 0.94776. The fitting results between PCF and cutting parameters are shown in Table 8, with all the P values less than 0.05, indicating that the fitting results are all credible.

3.7. Advantages of the Method. The existing roadway excavation technology has been relatively mature, but the hard rock roadway driving speed is slow and pick wear is serious, leading to cost increase. Reducing the cutting force is an effective means to reduce pick wear. By presplitting the rock and increasing the free surface, rock strength can be effectively reduced and the brittle fracture failure of the rock can be generated. According to the data in this paper, the influence of rock plate thickness on cutting force is the most obvious. The maximum thickness of granite studied in this paper is 30 mm, and the corresponding peak cutting force is 5.646 kn. In [5], 22 kinds of rocks are provided, in which the compressive strength of limestone is consistent with that of granite in this paper, which is 121 MPa. The tensile strength of granite in this paper is 12.1 MPa, harder than the limestone (7.8 MPa) in [5]. In the traditional rock breaking mode of continuous coal and rock, the cutting force required for breaking limestone is 29.4 kN when the cutting depth is 9 mm. According to [32], the ratio of peak cutting force to mean cutting force is 2.45 kN. The peak cutting force for limestone cutting should be 72.03 kN, which is far greater

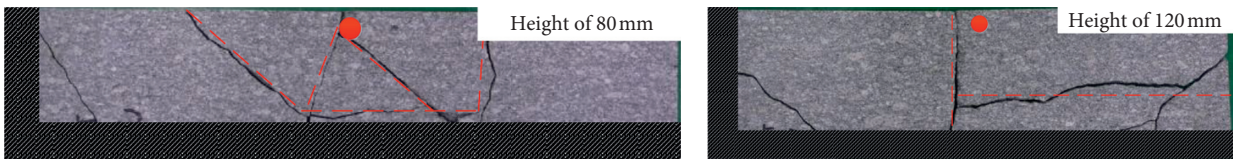

Figure 20: The cutting results with different height. (a) 80 mm and (b) 120 mm.

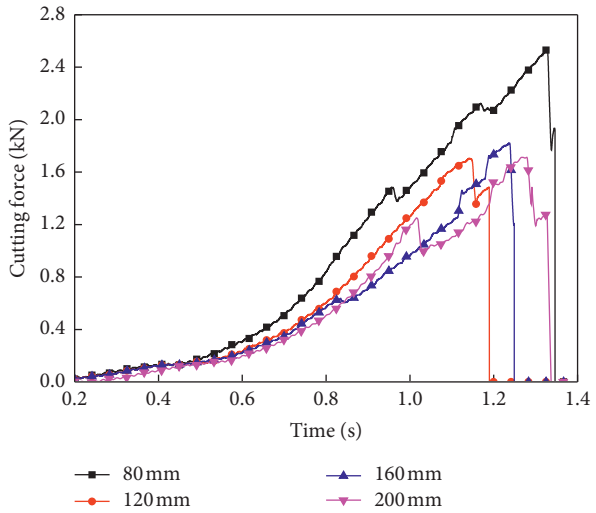

Figure 21: Variation in cutting force with time at different height.

Table 6: The PCF with different height of rock plate.

Height of rock plate (mm)	80	120	160	200
PCF (kN)	2.559	1.802	1.836	1.726

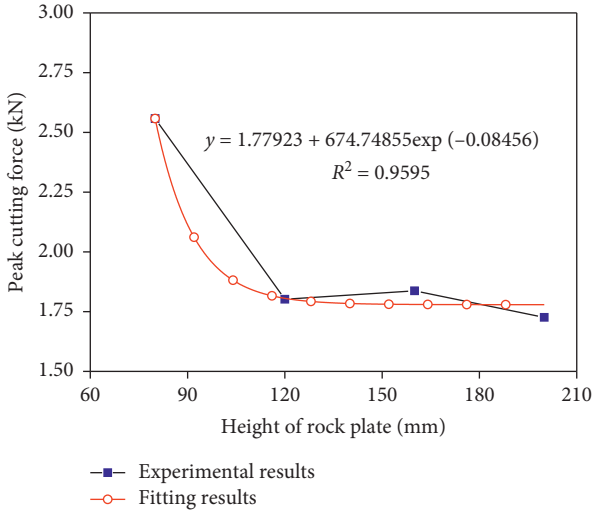

Figure 22: The relationship between PCF and height of rock plate.

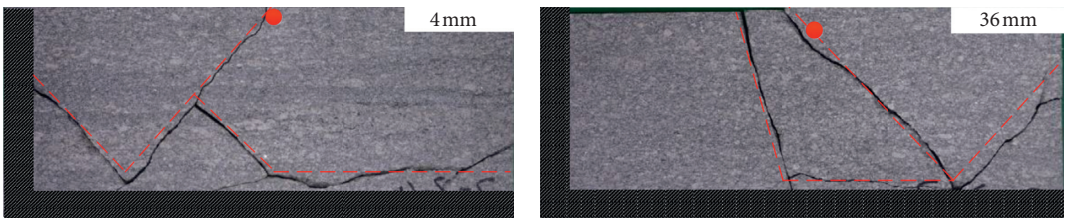

Figure 23: The cutting results of granite with different cutting depth. (a) 4 mm and (b) 36 mm.

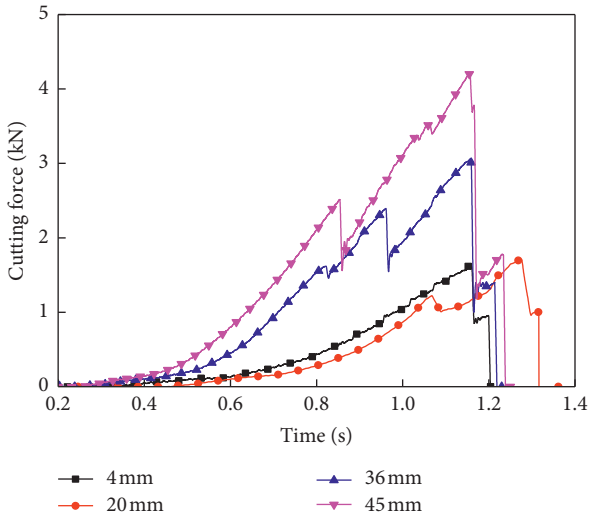

Figure 24: Variation in cutting force with time at different cutting depth.

Table 7: The PCF with different cutting depth.

Cutting depth (mm)	4	20	36	45
PCF (kN)	1.653	1.726	2.991	4.31

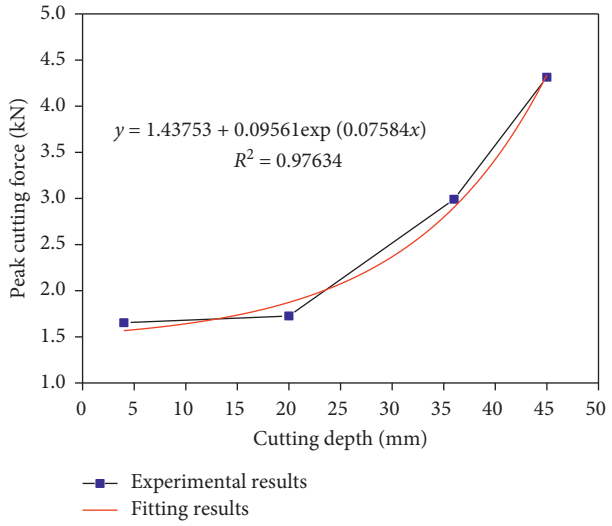

Figure 25: The relationship between PCF and cutting depth of conical pick.

Table 8: The fitting results between PCF and cutting parameters.

Variable	Fitting formula	R^2	P	Functional relationship
PCF-UCS	$y = -0.12287 + 0.14991x$	0.97356	0.009	Linear-positive
PCF-thickness	$y = 0.92159 + 0.01318\exp(0.1959x)$	0.99158	0.03	Exponential-positive
PCF-width	$y = 1.71628 + 11.52611\exp(-0.0185x)$	0.98847	0.005	Exponential-negative
PCF-height	$y = 1.77923 + 674.74855\exp(-0.08456)$	0.9595	0.02	Exponential-negative
PCF-cutting depth	$y = 1.34896 + 0.16122\exp(0.06223x)$	0.95028	0.04	Exponential-positive

than that of 5.646 kN when the granite thickness is 30 mm. Therefore, the method proposed in this paper can effectively reduce the cutting force and thus reduce the pick wear.

4. Conclusion

To increase the cutting performance and reduce the production cost, based on increasing free surface, a new rock cutting method is proposed. The cutting force and fracture morphology of rock plate are researched according to theoretical, numerical, and experimental methods:

(1) The foremost fracture position is deduced by theoretical method. The calculation results show that, at the cutting position and junction between free sides and fixed sides, rock plate breaks preferentially due to bore maximal bending moment and generated maximal deflection.

(2) Through numerical simulation of rock plate cutting, it can be seen that the rock plate had preferential fracture at the cutting position, with crack generated at the middle of rock plate, and the results are consistent with the theoretical value. Subsequently, the rock plate breaks at junction between free sides and fixed sides. After cracks connect with each other, rock plate separates from base rock. The numerical method employed in the paper is an effective method for rock plate cutting process.

(3) Under the constraint condition of rock plate with two sides fixed and two sides free, PCF increases linearly with the increasing UCS of rock plate, increases exponentially with the increasing thickness of rock plate and cutting depth of conical pick, and decreases exponentially with the increasing width and height of rock plate. The cutting depth of conical pick and thickness of rock plate influence PCF greater than width and height of rock plate. Besides, the peak cutting force produced by this method is obviously less than that of continuous coal and rock cutting.

(4) The size of rock fragments separated from base rock increases with the increasing UCS of rock. Higher width and height and lower cutting depth are more beneficial for rock cutting, due to generation of lower cutting force and occurrence of higher fracture area. Therefore, in the sawing process, rock plate with higher free surface area is more expected to be obtained.

Data Availability

The data used to support the findings of this study are included within the article.

Conflicts of Interest

The authors declare that they have no conflicts of interest.

Acknowledgments

This work was supported by the Natural Science Foundation of Shandong Province (Grant nos. ZR2019BEE069 and ZR2019MEE067) and the Key Research and Development Plan of Shandong Province (Grant no. 2019GGX104102).

References

[1] I. Evans, "A theory of the cutting force for point-attack picks," *International Journal of Mining Engineering*, vol. 2, no. 1, pp. 63–71, 1984.

[2] R. M. Goktan, "A suggested improvement on Evans' cutting theory for conical bits," in *Proceedings of the Fourth International Symposium on Mine Mechanization and Automation*, pp. 57–61, Queensland, Australia, July 1997.

[3] F. F. Roxborough and Z. C. Liu, "Teoretical considerations on pick shape in rock and coal cutting," in *Proceedings of the Sixth Underground Operator's Conference*, pp. 189–193, Kalgoorlie, Australia, November 1995.

[4] R. M. Goktan and N. Gunes, "A semi-empirical approach to cutting force prediction for point-attack picks," *The Journal of South African Institute of Mining and Metallurgy*, vol. 105, no. 4, pp. 257–263, 2005.

[5] N. Bilgin, M. A. Demircin, H. Copur, C. Balci, H. Tuncdemir, and N. Akcin, "Dominant rock properties affecting the performance of conical picks and the comparison of some experimental and theoretical results," *International Journal of Rock Mechanics and Mining Sciences*, vol. 43, no. 1, pp. 139–156, 2006.

[6] X. Wang, Q.-F. Wang, Y.-P. Liang, O. Su, and L. Yang, "Dominant cutting parameters affecting the specific energy of selected sandstones when using conical picks and the development of empirical prediction models," *Rock Mechanics and Rock Engineering*, vol. 51, no. 10, pp. 3111–3128, 2018.

[7] S. Wang, X. Li, K. Du, and S. Wang, "Experimental investigation of hard rock fragmentation using a conical pick on true triaxial test apparatus," *Tunnelling and Underground Space Technology*, vol. 79, pp. 210–223, 2018.

[8] J. Huang, Y. Zhang, L. Zhu, and T. Wang, "Numerical simulation of rock cutting in deep mining conditions," *International Journal of Rock Mechanics and Mining Sciences*, vol. 84, pp. 80–86, 2016.

[9] X. He, C. Xu, K. Peng, and G. Huang, "On the critical failure mode transition depth for rock cutting with different back rake angles," *Tunnelling and Underground Space Technology*, vol. 63, pp. 95–105, 2017.

[10] X. Wang and O. Su, "Specific energy analysis of rock cutting based on fracture mechanics: a case study using a conical pick on sandstone," *Engineering Fracture Mechanics*, vol. 213, pp. 197–205, 2019.

[11] L. Zhao, H. Liu, and W. Zhou, "A study on the dynamic transmission law of spiral drum cutting coal rock based on ANSYS/LS-DYNA simulation," *Complexity*, vol. 2019, pp. 1–14, 2019.

[12] P. L. Menezes, M. R. Lovell, I. V. Avdeev, J. Lin, and C. F. Higgs, "Studies on the formation of discontinuous chips during rock cutting using an explicit finite element model," *The International Journal of Advanced Manufacturing Technology*, vol. 70, no. 1-4, pp. 635–648, 2013.

[13] Y. Zhou and J.-S. Lin, "Modeling the ductile-brittle failure mode transition in rock cutting," *Engineering Fracture Mechanics*, vol. 127, pp. 135–147, 2014.

[14] J.-Y. Park, H. Kang, J.-W. Lee et al., "A study on rock cutting efficiency and structural stability of a point attack pick cutter by lab-scale linear cutting machine testing and finite element analysis," *International Journal of Rock Mechanics and Mining Sciences*, vol. 103, pp. 215–229, 2018.

[15] A. Wang, J. Liu, Z. Liu, Y. Xia, J. Xia, and S. Qiao, "Establishment of coal-rock constitutive models for numerical simulation of coal-rock cutting by conical picks," *Periodica Polytechnica Civil Engineering*, vol. 63, no. 2, pp. 456–464, 2019.

[16] S. Dewangan, S. Chattopadhyaya, and S. Hloch, "Wear assessment of conical pick used in coal cutting operation," *Rock Mechanics and Rock Engineering*, vol. 48, no. 5, pp. 2129–2139, 2014.

[17] X. Liu, P. Tang, Q. Geng, X. Li, and M. Tian, "Numerical research on wear mechanisms of conical cutters based on rock stress state," *Engineering Failure Analysis*, vol. 97, pp. 274–287, 2019.

[18] D. Yang, J. Li, L. Wang, K. Gao, Y. Tang, and Y. Wang, "Experimental and theoretical design for decreasing wear in conical picks in rotation-drilling cutting process," *The International Journal of Advanced Manufacturing Technology*, vol. 77, no. 9-12, pp. 1571–1579, 2014.

[19] Z. Lu, L. Wan, Q. Zeng, X. Zhang, and K. Gao, "Numerical simulation of rock plate cutting with three sides fixed and one side free," *Advances in Materials Science and Engineering*, vol. 2018, pp. 1–21, 2018.

[20] Z. Lu, Q. Zeng, Z. Meng, Z. Wang, and G. Gao, "Numerical simulation on cutting and fracturing of rock plate with one side fixed and three sides free," *Advances in Materials Science and Engineering*, vol. 2020, Article ID 8652637, 14 pages, 2020.

[21] Z. Lu, Q. Zeng, Z. Meng, Z. Wang, and G. Gao, "Numerical research on cutting force and fracture morphology of rock plate with two sides fixed and two sides free," *Mathematical Problems in Engineering*, vol. 2020, Article ID 2136297, 14 pages, 2020.

[22] H. Jeong, S. Choi, S. Lee, and S. Jeon, "Rock cutting simulation of point Attack picks using the smooth particle hydrodynamics technique and the cumulative damage model," *Applied Sciences*, vol. 10, no. 15, pp. 1–21, 2020.

[23] O. Su and M. Akkaş, "Assessment of pick wear based on the field performance of two transverse type roadheaders: a case study from Amasra coalfield," *Bulletin of Engineering Geology and the Environment*, vol. 79, no. 5, pp. 2499–2512, 2020.

[24] X. Liu and Q. Geng, "Effect of contact characteristics on the self-rotation performance of conical picks based on impact dynamics modelling," *Royal Society Open Science*, vol. 7, no. 5, pp. 1–14, 2020.

[25] W. Zhou, H. Wang, D. Wang, K. Zhang, Y. Du, and H. Yang, "The effect of geometries and cutting parameters of conical pick on the characteristics of dust generation: experimental investigation and theoretical exploration," *Fuel Processing Technology*, vol. 198, pp. 1–12, 2020.

[26] J. Zou, W. Yang, and J. Han, "Discrete Element Modeling of the Effects of Cutting Parameters and Rock Properties on Rock Fragmentation," *IEEE Access*, pp. 1–16, 2020.

[27] S. P. Timoshenko and S. Woinowsky-Krieger, *Theory of Plates and Shells*, McGraw-Hill, New York, NY, USA, 1959.

[28] S. P. Timoshenko and J. M. Gere, *Theory of Elastic Stability*, McGraw-Hill, New York, NY, USA, 1961.

[29] I. S. Sokolnikoff, *Mathematical Theory of Elasticity*, McGraw-Hill, New York, NY, USA, 1970.

[30] T. J. Holmquist, G. R. Johnson, and W. H. Cook, "A computational consititutive model for concrete subjected to large strains, high strain rates, and high pressures," in *Proceedings of the Fourteenth International Symposium on Ballistics*, pp. 1–10, Quebec City, Canada, September 1993.

[31] O. Su and N. Ali Akcin, "Numerical simulation of rock cutting using the discrete element method," *International Journal of Rock Mechanics and Mining Sciences*, vol. 48, no. 3, pp. 434–442, 2011.

[32] S. Yasar, "A general semi-theoretical model for conical picks," *Rock Mechanics and Rock Engineering*, vol. 53, no. 6, pp. 2557–2579, 2020.